https://doi.org/10.48048/tis.2024.8010

Understanding the Blood-Brain Barrier (BBB) with MRI Techniques and Its Implications in Neurodegenerative Diseases: An Overview

Cesare Oliveti[1], Aniello Iacomino[2], Francesco Manti[1], Emanuele Tinelli[1], Gianluca Gatta[3], Graziella Di Grezia[4], Giuseppe Lucio Cascini[1] and Vincenzo Cuccurullo[3,*]

[1]Department of Diagnostic Imaging, Magna Graecia University of Catanzaro, Catanzaro, Italy
[2]Department of Human Science, Guglielmo Marconi University, Rome, Italy
[3]Department of Precision Medicine, Università della Campania "Luigi Vanvitelli", Napoli, Italy
[4]Radiology Division, ASL Avellino, Avellino, Italy

([*]Corresponding author's e-mail: vincenzo.cuccurullo@unicampania.it)

Received: 29 January 2024, Revised: 19 March 2024, Accepted: 17 April 2024, Published: 10 July 2024

Abstract

The blood-brain barrier (BBB) stands as a critical guardian separating the central nervous system (CNS) from the systemic circulation. This comprehensive review explores the anatomical and functional components of the BBB and its association with the neurovascular unit (NVU), emphasizing its role in synaptic signaling and shielding the CNS from neurotoxic elements. Detailed discussions encompass MRI techniques like dynamic contrast enhancement (DCE) and arterial spin labeling (ASL) MRI, illuminating their significance in assessing BBB integrity and permeability. Various models and pharmacokinetic parameters utilized in imaging analysis offer insights into barrier permeability, aiding in the evaluation of neurodegenerative illnesses such as Alzheimer's, Parkinson's, and multiple sclerosis. Additionally, the study investigates the distinct characteristics of imaging protocols and their impact on BBB evaluation. Highlighting physiological conditions, the analysis discerns regional disparities in BBB permeability, shedding light on diverse microvascular architectures in healthy subjects. Conversely, in pathological states like Alzheimer's, Parkinson's, and multiple sclerosis, BBB dysfunction leads to a cascade of events facilitating the entry of harmful substances, exacerbating neurodegeneration. Imaging studies have unveiled distinct alterations in BBB permeability and perfusion, providing crucial insights into disease progression, notably preceding structural changes in Alzheimer's and indicating localized disruptions in multiple sclerosis. This comprehensive exploration underscores the pivotal role of the BBB in maintaining CNS health and its intricate involvement in the pathogenesis of neurodegenerative disorders. While imaging techniques serve as promising tools for BBB assessment, further research is warranted to refine their diagnostic precision and differentiation abilities across neurological conditions.

Keywords: Blood-brain barrier, Alzheimer's disease, Parkinson's disease, Multiple sclerosis, Dynamic contrast enanchement, Dynamic susceptibility contrast, Magnetic resonance imaging, Focused ultrasound

Introduction

The blood-brain barrier (BBB) is the main barrier system that separates the central nervous system (CNS) from the rest of the body. It's important to note 2 other barrier systems: The blood-cerebrospinal fluid barrier at the choroid plexus and the arachnoid barrier. Anatomically, the BBB consists of capillaries,

arterioles, and venules of the cerebral microvascular network. It is formed by brain endothelial cells (CECs) interconnected through tight junctions (TJ) [1]. The presence of TJ prevents water-soluble macromolecules from passively diffusing across the barrier through the para-cellular space. Trans-cellular diffusion across the luminal and ab-luminal surfaces of the BBB does not occur without specific transport proteins or by pinocytosis. CECs also interact with other cellular components such as pericytes through gap junctions, indicating a close functional relationship and communication through autocrine and paracrine signaling pathways. This communication is involved in the synthesis of proteins such as actin and the activation of vasoactive receptors.

Astrocytes play a significant role in supporting neurons by providing nutrients through intricate brain capillary networks they construct. Additionally, they regulate water transport via precise aquaporin-4 expression at their terminations, facilitating controlled water movement. Moreover, they secrete factors that, along with the basal membrane, promote the formation of tight junctions, reinforcing the integrity of the barrier. The basal membrane surrounds CECs and pericytes, providing structural support for the blood-brain barrier. Comprising collagen Type 4, elastin, fibrillin, laminin, and fibronectin alongside extracellular matrix proteins, cell adhesion molecules (CAM), and signaling proteins, it acts as a barrier, restricting the entry of foreign cells into the brain. Simultaneously, it creates a perivascular space that fosters a microenvironment for immune cell aggregation during inflammation [2].

These elements constitute the fundamental structural and functional unit of the blood-brain barrier (BBB), which is a critical component of the neurovascular unit (NVU). The concept of the NVU emphasizes the close developmental, structural, and functional association between brain cells and the microcirculation. It has been enthusiastically embraced by the scientific community due to its implications for normal brain function, particularly focusing on neurovascular signaling at the microcirculation level involving endothelial cells, mural cells (including vascular smooth muscle cells (SMCs) and pericytes), and astrocytic end-feet [3].

All these components (cells and basal membranes) enable the BBB to maintain a stable environment for neural function and preserve the optimal ionic composition for synaptic signaling through specific transporters [2]. The BBB helps to segregate central and peripheral transmitter pools and shields the CNS from circulating neurotoxic substances (metabolites, endogenous proteins, or xenobiotics) using energy-dependent efflux transporters ABC (ATP-dependent transporters) [4].

Magnetic resonance imaging of blood brain barrier

MRI techniques are the gold standard to assess the integrity of the BBB through contrast agent (CA) administration. Dynamic contrast enhancement (DCE) and dynamic susceptibility contrast (DSC) MRI are 2 approaches that utilize a gadolinium-based CA (**Figure 1**). Other approaches for measuring the integrity of the BBB use different mechanisms, including water exchange (Arterial Spin Labelling - MRI) [5]. We will only address DCE-MRI and ASL-MRI because our focus is on major neurodegenerative illnesses.

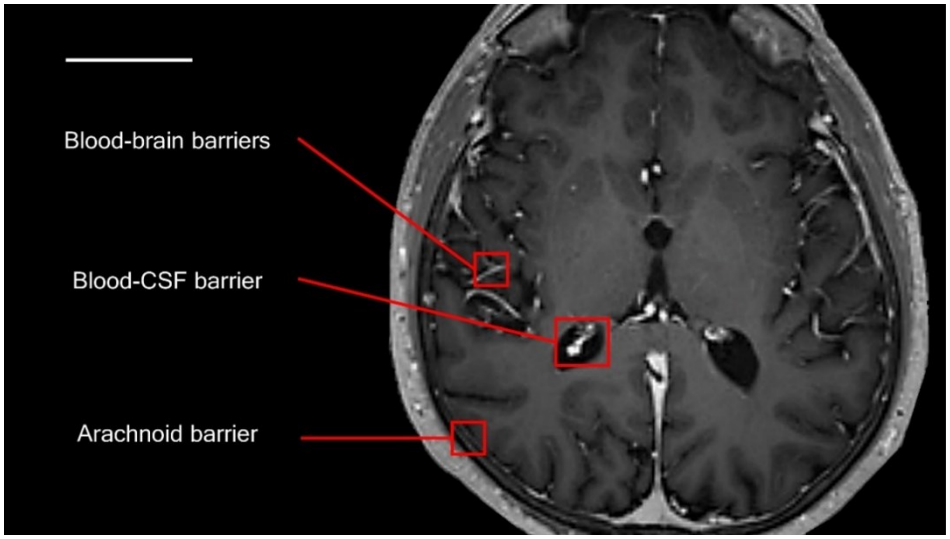

Figure 1 Schematic localization of the main biological barriers of the brain (MRI 3D-T1 weighted post-contrast axial image).

DCE-MRI

In pathological conditions affecting the blood-brain barrier (BBB), the contrast medium gathers in the tissue's extracellular and extra-vascular space (EES). This triggers a rise in longitudinal relaxation velocity, causing increased signal intensity in T1-weighted images. Using DCE-MRI, we can detect and assess any interruption in the BBB by observing this signal change. While DCE-MRI is the standard for permeability measurement, dynamic susceptibility contrast MRI (DSC-MRI) is preferred for perfusion imaging. However, DCE-MRI can blend both perfusion and permeability measures but requires a longer acquisition time to capture gradual interstitial impregnation and a high temporal resolution at the start to catch the initial pass of the contrast bolus [6].

Models and pharmacokinetic parameters

To assess and comprehend barrier permeability, tissue models must be created that allow the flow of contrast medium between blood plasma and the extracellular space to be described. Brix *et al.* [7], Larsson *et al.* [8], and Tofts [9], were the first to introduce pharmacokinetic modeling for DCE-MRI analysis, which was followed by a consensus publication on notation in the early 1990s. Improvements in imaging techniques (for example, improved temporal resolution and contrast-to-noise ratio) and a better understanding of the underlying physiology have aided the construction of more complicated pharmacokinetic models since then.

A few target parameters in DCE-MRI must be defined for this purpose, including fractional plasma volume (vp), fractional interstitial volume (ve), plasma flow (Fp), and the permeability-surface product (PS), which measures the rate at which contrast agent particles escape from the plasma into the EES per unit volume. Finally, we define Ktrans as a parameter of the rate at which the contrast agent is delivered to the EES per volume of tissue concentration and in arterial blood plasma. PS represents the clearance of contrast agent escaping from capillary plasma to the EES, the flow of contrast agent across the BBB normalized to tissue plasma concentration and tissue volume; in contrast, Ktrans is equal to the product of plasma flow Fp and extraction fraction E. (i.e., the fraction of contrast agent molecules escaping into the EES) [6].

Through the examination of the previously mentioned parameters: Fractional plasma volume vp, fractional interstitial volume ve, and permeability-surface product PS, "Tracer kinetic modelling" intends to demonstrate a correlation between a rise in tissue signal. The main models that allow the processing of contrast agent concentration curves in tissue are the following: (I) the modified Tofts model, (II) the Patlak model, and (III) the steady-state model.

Most pharmacokinetic models require identification of the arterial input function (AIF), which describes the tracer concentration in the blood plasma over time. Because each voxel of brain tissue should have a different form of contrast concentration input due to different vascular intake, AIF should be measured in small arterioles that supply blood to the tissue in each voxel that is being examined, but this becomes difficult for low spatial resolution without a partial volume effect (PVE) of the surrounding tissue, resulting in measurement ambiguity. An alternative measurement of AIF in a larger distal artery could be used, but this can cause secondary errors due to temporal delay and the spread of the bolus contrast agent. There is no solution to this contradiction, and a compromise is required. For example, if you are interested in studying patients with severe cerebrovascular disease, then it is more useful to measure AIF from a small proximal artery, although you sacrifice a certain degree of PVE errors. On the other hand, in pathologies without major arterial abnormalities (epilepsy, multiple sclerosis, etc.), then a large artery might be the best option.Therefore, the location (small or large artery) will depend on the pathology, study objectives, and clinical requirements that you want to examine through the MRI study [10].

The chosen kinetic model for assessing contrast agent permeation through the blood-brain barrier (BBB) depends on the level of impairment. Under normal conditions or mild BBB issues, the Patlak model is accepted as the most suitable for estimating Ktrans, the transfer constant of the agent from blood to brain. This model assumes the agent's access to 2 compartments separated by the BBB, limiting extravasation while maintaining predominant blood flow over permeability. However, in cases of significant BBB disruption, Ktrans values may rely on factors such as blood flow and permeability, not solely representing permeability. Pathological conditions might entail variations in vessel sizes, complicating result interpretation. Despite methods to assess permeability independently from blood flow, such as calculating the exchange rate (kGad), the validity of these measures isn't fully clear, especially in conditions assuming negligible efflux of the indicator in the bloodstream. In more severe BBB impairment, alternative models like the extended Tofts, considering more relevant efflux, might prove more accurate [11].

Characteristics of imaging protocols

The DCE-MRI procedure typically begins with the acquisition of images under baseline conditions, followed by the acquisition of T1-weighted images after an intravenous injection of contrast agent. By studying the kinetics of contrast impregnation and measuring the variation of signal intensity as a function of time, quantitative or semi-quantitative information on the integrity of the BBB can be extracted. There is no standardized MRI protocol in readout, but different protocols are used in different ways. Spoiled gradient echoes and ultrafast sequences are the most used sequences. TOMROP (T-One by Multiple Read-Out Pulses), T1 mapping of partial inversion recovery (TAPIR), the THRIVE sequence, RF-FAST, and TWIST are less commonly used.

Furthermore, most human studies used mid-field strength MRI machines (1.5 T), with a minority of studies using high-field scanners (3.0 T); this is likely due to the greater availability of mid-field machines in the area. In animal studies, a wider range of 1.5 to 11.75 T magnetic field strength is used.

The most used contrast agent was Gd-DTPA (gadopentetate dimeglumine) or its variant Gd-DTPA-BMA (gadodiamide), which was administered intravenously in the standard dose of 0.1 mmol/kg body weight. Although the doses administered ranged from 0.02 to 0.5 mmol/kg. Other studies have used

gadolinium-based agents such as Gd-DOTA (gadoterate meglumine) and gadobutrol (Gd-BT-DO3A). However, no studies have been conducted to determine how much the variability of different types or concentrations of contrast agents can influence increasing or decreasing the signal-to-noise ratio.

The duration of the examination also varies greatly, ranging from 2.1 to 155 min. It should be noted that the shorter scan time and lower temporal resolution result in higher uncertainty in the pharmacokinetic parameters Ktrans, ve, and vp. The duration of the examination varied according to the pathology studied, with longer times for tumor pathology. Studies examining tissues undergoing slower structural functional loss processes (tissues appearing healthy in MS, aging, or dementia) had a lower temporal resolution [6].

Arterial spin labeling - MRI

Measurement of water exchange using MRI with arterial spin labeling (ASL) holds promise as a potential marker of blood-brain barrier (BBB) impairment because low sensitivity of DCE-MRI in studying water exchange across the blood-brain barrier. It highlights that water, being a smaller molecule, can traverse this barrier differently compared to GBCAs, exhibiting greater sensitivity to subtle changes in the barrier structure. Three main measurement approaches are employed, aiming to detect the effects of barrier-crossing on detectable nuclear magnetic resonance parameters like T1, T2, ADC. Contrast agent-based techniques enhance sensitivity by detecting bi-exponential relaxation, enabling estimation of the water-tissue exchange rate. These approaches also allow for the calculation of cerebral blood volume and the permeability surface area product, offering quantitative measures of water exchange [11].

Water, moving through the BBB via both passive and active diffusion mechanisms, exhibits slower transfer rates compared to gadolinium due to its smaller molecular weight and size. ASL stands out as a versatile technique for studying various BBB pathologies. ASL employs magnetic labeling (reversing magnetization) of incoming blood. It evaluates the ASL signal by measuring the signal difference between images acquired before and after the labeling of incoming blood, as the magnetically labeled spin traverses the brain in the imaging plane for a duration defined by the delay time of the subsequent labeling.

The measured position of the labeled magnetization over time, influenced by relaxation times, diffusivity between intravascular and extravascular compartments, and exchange of labeled protons with water spins, allows quantification of water exchange rates between these compartments. Calculating the permeability surface water product of the BBB (PSw) involves utilizing the fractional blood volume (vb) and the rate of water exchange from blood to brain (kin). A comprehensive understanding of the impact of multiple compartments on T1, T2, and diffusion, crucial for permeability parameters, may necessitate integrating several methodologies (such as kin and PSw). Advanced multi-compartmental models may extract the water exchange signal from the total signal using compensation techniques, enabling accurate measurements of water exchange at the BBB [5].

The arterial spin labeling (ASL) technique allows monitoring labeled water and determining its localization (intravascular or extravascular) over post-labeling time. ASL variations, such as adding T2/T2* weights or diffusion techniques, enhance label localization and enable assessment of water exchange. Multi-echo time ASL (Multi-TE) techniques estimate the behavior of labeled spins over time, suggesting that prolonged post-labeling times are associated with a longer T2 environment in the extravascular area. This aids in calculating the pre-exchange water duration but necessitates accurate measurement of arterial transit time (ATT). However, variability in tissue/blood T2 based on oxygenation might complicate inter-study comparisons.

Diffusion-weighted ASL (DW-ASL) exploits diffusion differences between vascular and extravascular compartments to quantify label proportions in each compartment based on post-labeling time. There are also double diffusion encoding methods based on diffusion-exchange spectroscopy (DEXSY),

known as filter-exchange imaging (FEXI), which do not require contrast agents and aim to utilize natural differences in water diffusion between vascular and extravascular compartments.

Lastly, intravoxel incoherent motion uses spin perfusion in intravascular compartments as isotropic diffusion. This method aims to measure transcytolemmal water exchange and across the blood-brain barrier, showing promising results in detecting exchange rates similar to those obtained with other techniques [11]. Preclinical investigations have demonstrated the sensitivity of this method. In comparison to traditional DCE-MRI, studies evaluating BBB permeability using ASL and DCE techniques indicated ASL's ability to detect subtle changes in the BBB. ASL studies in AD mice revealed BBB alterations, contrasting with DCE-MRI's absence of leakage. Wang's *et al.* [5] approach showcased a robust evaluation of cerebral perfusion in human studies.

Additionally, a positive correlation emerged between kw and Ktrans in white matter (WM), the middle cerebral artery (MCA) perforating region, and the caudate, as well as between kw and k Gad in the MCA perforating territory, hippocampus, and medial temporal lobe, when comparing the rate of water exchange across the BBB with Ktrans and k Gad. Thus, kw emerges as a reliable measure for assessing the rate of water exchange across the BBB, offering a consistent test-retest measure [12].

Models and pharmacokinetic parameters

The original ASL models were founded on the single-compartment Kety model, which inaccurately assumed immediate exchange of all labeled water from the capillary to the extravascular space ($PSw \rightarrow \infty$). Applying a single-compartment model to ASL data can result in substantial errors, up to 62 % in cerebral blood flow (CBF), especially in white matter (WM). As a solution, two-compartment models have been developed.

The general two-compartment exchange model proposed by Zhou's *et al.* [13], incorporates the slow-flow approximation, assuming that the magnetization difference of venous blood equals zero ($\Delta Mv = 0$), and the single-pass approximation (SPA), assuming the label doesn't have sufficient time to re-enter the blood compartment before measurement.

In contrast, the Alsop *et al.* [14] model introduces an 'ad hoc' vascular compartment. Unlike the general two-compartment model, the input to the extravascular compartment mirrors that of the vascular compartment. Consequently, the difference in magnetization of the capillary blood equals that of the extravascular space ($\Delta Mb = \Delta Ma$). Wilson's *et al.* [15], general tissue homogeneity model predicts the vascular space as a plug flow rather than a well-mixed compartment. Common approximations using time domain solutions encompass SPA and the adiabatic approximation to tissue homogeneity (AATH).
Furthermore, the stepwise model, Li's *et al*. [16], 4-step capillary model, considers transit through larger vessels without exchange [12].

What the mri revealed in physiological conditions

Imaging studies have provided insights into barrier permeability, revealing distinctive patterns in both healthy and pathological conditions. In one study, contrasting permeability levels were highlighted in specific brain areas of healthy subjects following the administration of a contrast agent. Notably, the hippocampus exhibited a significantly higher concentration of the contrast agent than other regions, indicating heterogeneous permeability due to unique microvascular architecture and protein expression. The hippocampus, distinguished by its anatomy and blood supply, draws from both the anterior and posterior circulation [17].

Similarly, another study involving healthy elderly subjects observed regional variations in barrier permeability, particularly in grey matter nuclei such as the hippocampus. Intriguingly, these differences weren't associated with age, cognitive scores, or vascular risks [18].

Histological examinations supported these findings by illustrating a higher vascular volume in grey matter compared to white matter. The greater capillary density in grey matter reflects diverse metabolic needs, influencing the exchange of water, oxygen, nutrients, and solutes within the brain microcirculation [19].

These variations in morphology, cellular composition, and microvascular density, particularly between white and grey matter, imply nuanced heterogeneity that impacts the neurovascular unit and vascular tree across various brain regions [20].

BBB in pathological conditions

The analysis of the BBB is of great importance because the dysfunction of this dynamic system acts in the pathogenesis of neurodegenerative diseases [21].

Alzheimer' disease

AD, the most common neurodegenerative disorder, involves the accumulation of amyloid beta peptides (Aβ) and neurofibrillary tangles in the brain. The BBB is crucial because it regulates the movement of Aβ across it, thanks to specific proteins like RAGE, LRP1, and P-gp, which control Aβ flow into and out of the brain.

In AD, an increase in Aβ movement into the brain (by RAGE) and a decrease in its removal (by LRP1 and P-gp) cause Aβ to accumulate in the brain. Studies in animal models show BBB damage mainly around plaque-surrounded microvessels. According to the "2 Blows" theory, initial damage to blood vessels triggers BBB dysfunction, reducing its ability to keep harmful substances out, leading to reduced blood flow in the brain, neuronal damage, and increased Aβ in AD.

Lifestyle factors can independently or together contribute to damage in brain blood vessels, furthering Aβ accumulation. This damage includes reduced GLUT1 (which transports glucose), early blood vessel deterioration, decreased blood flow, and more BBB damage, worsening AD.

Changes in the BBB contribute to AD progression. This includes altered levels of specific proteins involved in Aβ movement, such as increased RAGE, decreased LRP1, reduced GLUT1, weakened tight junctions, decreased MFSD2A or increased caveolin-1, lowered P-gp, and degradation of the basal lamina via MMP9 [22].

Parkinson disease

PD, the second most prevalent neurodegenerative condition, is characterized by synuclein proteins' accumulation, forming Lewy bodies or cytoplasmic eosinophilic inclusions, alongside dopaminergic neurodegeneration.

The BBB's pivotal role in PD's pathophysiology is evident when impaired at the basal ganglia level. This impairment triggers a cascade leading to the accumulation of substances like fibrin, thrombin, plasmin, and red blood cells (RBCs), accompanied by the release of hemoglobin and iron. Consequently, this sequence generates reactive oxygen species (ROS), creating a hostile environment detrimental to dopaminergic neurons.

Furthermore, the compromised BBB facilitates the passage of α-synuclein, a pivotal protein in PD pathology, into the brain. The observed elevation in the α-synuclein efflux transporter (LRP1) in PD, akin to its increase in Alzheimer's disease (AD), hints at a potential mechanism for more efficient α-synuclein

removal or clearance. This heightened LRP1 activity might influence the regulation of α-synuclein levels, potentially impacting the course of PD.

Additionally, the reduction in tight junctions (TJs) of ZO1 and occludin within the striatal BBB in mouse studies bears significant implications for PD. This decrease in TJs signifies compromised barrier integrity in the striatum, potentially facilitating the passage of substances or molecules contributing to PD pathology [23].

Mulitiple sclerosis

The compromised Blood-Brain Barrier (BBB) in MS leads to crucial consequences. When the BBB's integrity is compromised, it allows activated lymphocytes entry into the peripheral central nervous system (CNS), initiating a localized immune response. This immune response involves the release of various inflammatory substances, including cytotoxic agents, pro-inflammatory cytokines, matrix metalloproteases, and reactive oxygen and nitrogen radicals by activated glial cells and infiltrating leukocytes.

These substances further compromise the BBB's integrity, exacerbating the immune response and perpetuating damage to the CNS [24]. Recent studies have associated changes in the composition of tight junctions (TJ) with BBB dysfunction, indicating various factors contributing to this impairment [25].

Moreover, the expansion of Virchow-Robin spaces observed during MS holds significance. These spaces serve as alternative lymphatic routes, containing inflammatory cells that act as auxiliary lymphatic vessels. This process aids in clearing antigens and immune cells away from affected CNS areas. The observed expansion suggests the body's attempt to manage the immune response in MS by utilizing these spaces as supplementary channels for antigen clearance [24].

Fibrinogen accumulation within veins, independent of lesion presence, indicates a consistent association with MS progression. Research shows more substantial fibrinogen loss in lesions of longer duration, implying a greater propensity for its depletion as lesions persist. Additionally, fibrinogen's presence within astrocytic and axonal structures implies its involvement in astrocyte and neuron interactions within the CNS in MS cases. This accumulation, along with its localization within astrocytic and axonal structures, suggests a potential role in ongoing inflammation, lesion development, and MS progression.

Altered BBB permeability proves to be crucial in MS pathophysiology, remaining or reoccurring in later stages of the disease. This BBB dysfunction, combined with leukocyte trans-endothelial migration, represents the initial brain abnormality in MS [25].

What the MRI revealed in pathological conditions

Additionally, applying semi-quantitative and quantitative evaluation systems is beneficial in studying various pathological conditions (**Figure 2**) [26].

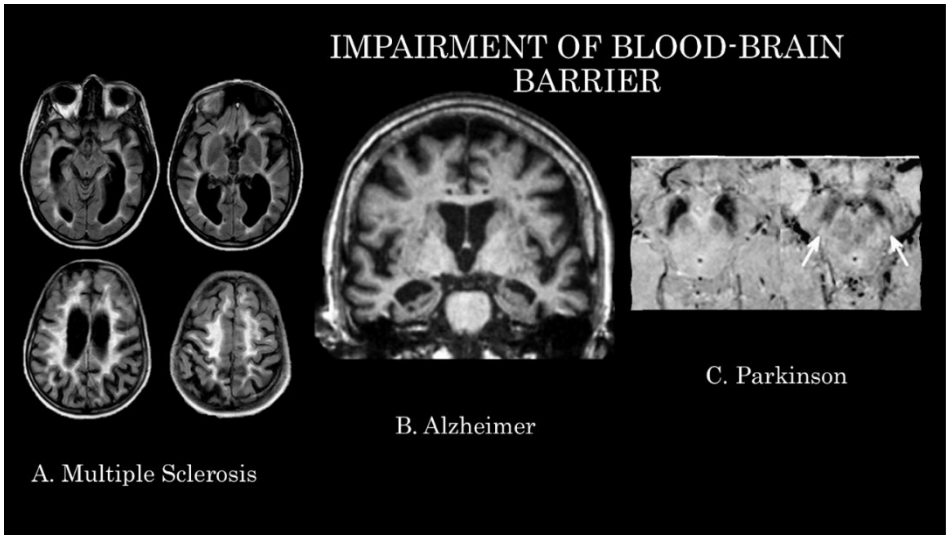

Figure 2 MRI features in advanced stages of neurodegenerative diseases: (A) Multiple sclerosis: FLAIR axial images show multiple demyelinating hyperintense lesions in the white matter; (B) Alzheimer's disease: 3D- T1 weighted coronal image shows bilateral atrophy of the hippocampus more evident on the right side; (C) Parkinson' disease: SWI axial images show, on the right, the absence of the nigrosome 1 in a PD patient, on the left, arrows indicate the nigrosomes 1 in a normal subject.

In the investigation of demyelinating conditions like Multiple Sclerosis, dynamic contrast-enhanced MRI (DCE-MRI) employing the Patlak model allows a quantitative evaluation of permeability and perfusion characteristics in demyelinated lesions and unaffected white matter regions. MRI biomarkers such as Ktrans, Vp, CBF, and CBV demonstrate notably higher values in contrast-enhancing lesions compared to non-enhancing ones. Interestingly, these parameters don't significantly differ from those in normal white matter [27]. ASL-MRI studies identify changes in the normal blood-brain barrier (BBB) function, resulting in reduced water exchange in relapsing-remitting MS patients, indicating compromised neuronal metabolic activity [28].

Moreover, BBB alterations may lead to decreased cerebral blood flow (CBF) observed in specific brain areas like the frontal cortex, thalamus, and caudate in patients, without evident loss of gray matter volume or cortical thickness reduction. These methodologies enable the early detection of alterations even in the absence of structural volumetric changes [29]. This reflects documented permeability changes in post-mortem studies where fibrinogen deposition indicates barrier alteration and the presence of various inflammatory cells. Active lesions demonstrate an accumulation of leukocytes and T cells in the perivascular spaces, both in chronic active lesions and around them [30].

In the realm of neurodegenerative pathology, dynamic contrast-enhanced MRI studies have observed changes in permeability within the medial temporal lobe (MTL) and hippocampus among individuals with mild cognitive impairment (MCI). In these instances, Ktrans evaluation was conducted using the Patlak analysis method. Notably, such barrier alterations precede the typical brain atrophy observed at the onset of Alzheimer's disease (AD) [31]. Intriguingly, researchers have showcased that vascular loss in the MTL acts as an early independent marker of cognitive decline unrelated to beta-amyloid and tau pathology. Furthermore, BBB loss in white matter significantly increases in individuals with MCI, where the primary cause of cognitive decline is vascular pathology, suggesting that localized BBB disruption might initiate lesions, elucidating the decrease in information processing speed [32].

It's believed that BBB rupture in MCI isn't an isolated phenomenon; vascular risks induce BBB impairment at various molecular levels, discernible using tracers of varying sizes. Water extraction using arterial spin labeling MRI with phase contrast (WEPCAST) measured BBB permeability to water molecules in older individuals, both with and without cognitive decline.

Additionally, compared to cognitively healthy subjects, the BBB in MCI patients exhibited higher permeability to small molecules like water than to larger ones like albumin. The permeability of BBB to water correlates with AD markers in CSF, Aβ, and tau. Conversely, BBB permeability to albumin relates to vascular risk factors but not to AD pathology. Notably, BBB permeability to small molecules, not large ones, predicted cognitive function. These findings suggest that BBB disruption is linked to both AD and vascular risks but showcases distinct effects. BBB permeability to small molecules has a more pronounced impact on cognitive performance.

The heightened BBB permeability to water may also signify dysregulation of aquaporin-4 channels (AQP4), as confirmed in DCE-MRI studies showing increased BBB permeability in the MTL in MCI. Both increased AQP4 expression and reduced AQP4 polarization have been noted in aging and AD, potentially affecting water permeability differently [33]. Recent mouse studies demonstrate changes in BBB permeability to water during aging using multi-echo-time arterial spin labeling MRI. These studies observed a 32 % faster BBB water permeability in older mice associated with aquaporin-4 water channel RNA expression [31].

The dynamic contrast-enhanced magnetic resonance imaging (DCE MRI) and arterial spin labeling magnetic resonance imaging (ASL MRI) both emerge as promising diagnostic tools for assessing blood-brain barrier (BBB) compromise, especially in Alzheimer's disease (AD). However, they come with limitations: DCE MRI can distinguish disease-specific BBB compromise but has limitations in early use due to contrast agent sizes; ASL MRI, though more sensitive to subtle BBB changes, has reduced capacity to detect compromise in smaller regions like the hippocampus. ASL MRI, using water as a tracer, can detect finer changes but requires further studies to fully understand the varied impacts on the BBB in AD pathology. Both techniques show significant associations with biological markers and potentially predict AD progression, but they aren't yet definitive standalone diagnostic tools. Ultimately, while these methodologies offer significant prospects, further research is needed to optimize their ability to differentiate AD-related BBB compromise from other neurological conditions and to become more reliable and comprehensive diagnostic tools [34].

In Parkinson's disease, DCE-MRI studies showcase increased gadolinium passage in the basal ganglia, indicating disrupted normal barrier function [35,36]. Meanwhile, several ASL-MRI studies note altered barrier permeability and reduced perfusion in posterior cortical regions compared to controls [37].
Table 1 The advancement of brain imaging techniques shows promise for neurovascular research, allowing investigation of BBB integrity in small regions like hippocampal subfields using high-power 7 T magnets. These techniques detect vascular changes including regional cerebral blood flow reductions, hemodynamic responses, enlarged perivascular spaces, and microhemorrhages. BBB imaging, coupled with focused ultrasound (FUS) guided by MRI, facilitates selective drug administration. MRgFUS, undergoing clinical trials for various neurological disorders, combines with intravenous microbubble injections to temporarily open the BBB, enhancing delivery of potential disease-modifying therapies. Animal studies suggest benefits in AD, potentially removing amyloid-beta from the brain. MRgFUS emerges as a promising approach for treating MCI and targeting pathology-associated brain regions in PD, possibly slowing dementia progression [38].

Alternative imaging techniques

Positron emission tomography (PET) and single-photon emission computed tomography (SPECT) are nuclear imaging techniques, which sacrifice some spatial resolution but have exquisite sensitivity and are considered gold standard techniques for *in vivo* imaging of transport mechanisms such as P-gp-mediated efflux, and GLUT1-mediated glucose uptake from the blood [35,39]. In particular, today PET has opened the doors to modern molecular imaging which allows us to trace and quantify pathophysiological processes and link them to pathologies at the cellular level [40]. 3 types of radiotracers have been developed: Efflux transporter substrates, inhibitors, and pro-drugs [41-43].

These techniques typically quantify the pharmacokinetics of a radiolabeled drug that is injected at tracer (subpharmacological) doses and that binds with high affinity to a specific receptor target [44]. Through modeling, pharmacokinetic parameters are then used to determine the so-called binding potential of the receptor site; the binding potential is the product of receptor density and the affinity of the radioligand for the receptor [36,45,46].

Limit

The primary constraint of permeability techniques lies in the wide variability of quantitative values derived from these measurements. Recent studies have showcased a spectrum of BBB permeability values ranging from 2.3×10^{-6} to 2.19×10^{-3} min^{-1}. Overall, Ktrans values were consistent with earlier studies as reported by Cramer *et al*. and Yoo *et al.* [38,47]. Conversely, van de Haar *et al*. [48], Ivanidze *et al.* [17]., Chi *et al.* [49] and Kim *et al.* [50]. documented notably lower Ktrans values. These discrepancies among studies may be attributed to the use of different models for computing Ktrans, particularly when dealing with subtle changes in barrier permeability [47,48,51,52].

For instance, studies employing the Patlak model reported significantly higher Ktrans values compared to those using the extended Tofts model, observed in Chi *et al.* [49], and Ivanidze *et al.* [17]. While the extended Tofts model remains favorable in brain tumor imaging, its applicability in evaluating neurodegenerative diseases or small vessel diseases necessitates further justification. Hence, recommending the Patlak model as the optimal pharmacokinetic model for DCE imaging analysis of subtle changes in BBB permeability, particularly in neurodegenerative diseases, is advisable. This model exhibits a high contrast-noise ratio for Ktrans and, unlike the extended Tofts model, requires fewer parameters, thereby reducing overfitting in low permeability environments. Moreover, simplified one-dimensional simulations strongly indicate that various factors such as noise, scanner drift, model assumptions, and spatio-temporal effects like coarse motion, k-sampling space, and movement artifacts can introduce errors in estimating permeability [23].

Another consideration pertains to the choice of MRI techniques employed in studying changes in BBB permeability. Arterial Spin Labeling (ASL), like any imaging examination, is highly sensitive to artifacts: Motion, signal interruption, distortion, bright spots, and labeling errors. Metallic surgical materials and hemorrhage also contribute to such artifacts. Bright spots are random clusters of voxels with very high perfusion due to residual vascular signal. Failure to label incoming blood leads to an apparent lack of perfusion in the affected vascular territory. ASL should not be performed after administering gadolinium-based contrast agents, as the resulting T1 shortening is detrimental to labeling. Therefore, adhering to standard protocols during perfusion measurement and minimizing the influence of wakefulness/ consciousness, satiety, acute substance use, and certain medications is crucial [37].

Table 1 studies illustrating evidence of blood-brain barrier (BBB) disruption on neuroimaging in neurodegenerative disorders.

References	Disease	Imaging techniques	Results
Xiong *et al.* [27].	Multiple sclerosis	DCE - MRI	The Ktrans, Vp, CBF, and CBV of CE lesions were significantly higher than that of NE lesions,
Rooney *et al.* [28].		ASL - MRI	Metabolic deficits and changes in sodium-potassium pump activity, and thus in BBB, are highlighted in the various brain regions affected by MS.
De La Pena *et al.* [29].		ASL - MRI	early perfusion changes in MS can be assessed even in those with absent or minimal structural changes
Chagnot *et al.* [32].	Alzheimer' disease	DCE-MRI	DCE-MRI underlined the occurrence of local, subtle, and progressive BBB leakage in aging.
Lim *et al.* [18-48].		ASL-MRI	Increased water permeability in MCI patients correlates with AD, indicating a distinct BBB breakdown between AD and vascular risks, crucial in both conditions.
Ohene *et al.* [31].		ASL-MRI	Age-related changes to water permeability across the BBB
Lee *et al.* [34].		DCE and ASL - MRI	BBB imaging shows that subtle BBB breakdown in preclinical AD can resemble that in healthy aging due to neuroinflammation or other neurological disorders.
Melzer *et al.* [51].	Parkinson's disease	ASL-MRI	A distinct perfusion network associated with Parkinson's disease characterized by decreased cortical perfusion

References

[1] I Wilhelm, A Nyul-Toth, M Suciu, A Hermenean and IA Krizbai. Heterogeneity of the blood-brain barrier. *Tissue Barriers* 2016; **4**, e1143544.

[2] PM Carvey, B Hendey and AJ Monahan. The blood-brain barrier in neurodegenerative disease: A rhetorical perspective. *J. Neurochem.* 2009; **111**, 291-314.

[3] S Schaeffer and C Iadecola. Revisiting the neurovascular unit. *Nat. Neurosci.* 2021; **24**, 1198-209.

[4] NJ Abbott, AAK Patabendige, DEM Dolman, SR Yusof and DJ Begley. Structure and function of the blood-brain barrier. *Neurobiol. Dis.* 2010; **37**, 13-25.

[5] PE Elschot, WH Backes, AA Postma, RJV Oostenbrugge, J Staals, RPW Rouhl and JFA Jansen. A Comprehensive View on MRI Techniques for Imaging Blood-Brain Barrier Integrity. *Invest. Radiol.* 2021; **56**, 10-19.

[6] AK Heye, RD Culling, MDCV Hernandez, MJ Thrippleton and JM Wardlaw. Assessment of blood-brain barrier disruption using dynamic contrast-enhanced MRI. A systematic review. *NeuroImage Clin.* 2014; **6**, 262-74.

[7] G Brix, W Semmler, R Port, LR Schad, G Layer and WJ Lorenz. Pharmacokinetic parameters in CNS Gd-DTPA enhanced MR imaging. *J. Comput. Assist. Tomogr. Luglio.* 1991; **15**, 621-8.

[8] HBW Larsson, M Stubgaard, JL Frederiksen, M Jensen, O Henriksen and OB Paulson. Quantitation of blood-brain barrier defect by magnetic resonance imaging and gadolinium-DTPA in patients with multiple sclerosis and brain tumors. *Magn. Reson. Med. Ottobre.* 1990; **16**, 117-31.

[9] PS Tofts and AG Kermode. Measurement of the blood-brain barrier permeability and leakage space using dynamic MR imaging. 1. Fundamental concepts. *Magn. Reson. Med. Febbraio.* 1991; **17**, 357-67.

[10] F Calamante. Arterial input function in perfusion MRI: A comprehensive review. *Prog. Nucl. Magn. Reson. Spectrosc. Ottobre.* 2013; **74**, 1-32.

[11] WJ Harris, M Asselin, R Hinz, LM Parkes, S Allan, I Schiessl, H Boutin and BR Dickie. *In vivo* methods for imaging blood-brain barrier function and dysfunction. *Eur. J. Nucl. Med. Mol. Imaging* 2023; **50**, 1051-83.

[12] BR Dickie, GJM Parker and LM Parkes. Measuring water exchange across the blood-brain barrier using MRI. *Prog. Nucl. Magn. Reson. Spectrosc.* 2020; **116**, 19-39.

[13] J Zhou, DA Wilson, JA Ulatowski, RJ Traystman and PCMV Zijl. Two-compartment exchange model for perfusion quantification using arterial spin tagging. *J. Cereb. Blood. Flow. Metab. Aprile.* 2001; **21**, 440-55.

[14] DC Alsop and JA Detre. Reduced transit-time sensitivity in noninvasive magnetic resonance imaging of human cerebral blood flow. *J. Cereb. Blood. Flow. Metab. Novembre.* 1996; **16**, 1236-49.

[15] JA Johnson, TA Wilson. A model for capillary exchange. *Am. J. Physiol.* 1966; **210**, 1299-303.

[16] K Li, X Zhu, N Hylton, G Jahng, MW Weiner and N Schuff. Four-phase single-capillary stepwise model for kinetics in arterial spin labeling MRI. *Magn. Reson. Med. Marzo.* 2005; **53**, 511-8.

[17] J Ivanidze, M Mackay, A Hoang, JM Chi, K Cheng, C Aranow, B Volpe, B Diamond and PC Sanelli. Dynamic contrast-enhanced mri reveals unique blood-brain barrier permeability characteristics in the hippocampus in the normal brain. *AJNR Am. J. Neuroradiol.* 2019; **40**, 408-11.

[18] IH Ha, C Lim, Y Kim, Y Moon, S Han and W Moon. Regional differences in blood-brain barrier permeability in cognitively normal elderly subjects: A dynamic contrast-enhanced MRI-based study. *Korean J. Radiol.* 2021; **22**, 1152.

[19] A Varatharaj, M Liljeroth, A Darekar, HBW Larsson, I Galea and SP Cramer. Blood-brain barrier permeability measured using dynamic contrast-enhanced magnetic resonance imaging: A validation study. *J Physiol. Febbraio.* 2019; **597**, 699-709.

[20] A Villabona-Rueda, C Erice, CA Pardo and MF Stins. The evolving concept of the blood brain barrier (BBB): From a single static barrier to a heterogeneous and dynamic relay center. *Front. Cell. Neurosci.* 2019; **13**, 405.

[21] G McCaffrey and TP Davis. Physiology and pathophysiology of the blood-brain barrier: P-glycoprotein and occludin trafficking as therapeutic targets to optimize central nervous system drug delivery. *J. Investig. Med.* 2012; **60**, 1131-40.

[22] MD Sweeney, AP Sagare and BV Zlokovic. Blood-brain barrier breakdown in Alzheimer disease and other neurodegenerative disorders. *Nat. Rev. Neurol.* 2018; **14**, 133-50.

[23] L Han and C Jiang. Evolution of blood-brain barrier in brain diseases and related systemic nanoscale brain-targeting drug delivery strategies. *Acta Pharm. Sin. B* 2021; **11**, 2306-25.

[24] GG Ortiz, FP Pacheco-Moisés, MÁ Macías-Islas, LJ Flores-Alvarado, MA Mireles-Ramírez, ED González-Renovato, VE Hernández-Navarro, AL Sánchez-López and MA Alatorre-Jiménez. Role of the blood-brain barrier in multiple sclerosis. *Arch. Med. Res.* 2014; **45**, 687-97.

[25] CMP Vos, JJG Geurts, L Montagne, ESV Haastert, L Bö, PVD Valk, F Barkhof and HED Vries. Blood-brain barrier alterations in both focal and diffuse abnormalities on postmortem MRI in multiple sclerosis. *Neurobiol. Dis.* 2005; **20**, 953-60.

[26] AK Heye, MJ Thrippleton, PA Armitage, MDC Valdes Hernandez, SD Makin, A Glatz, E Sakka and JM Wardlaw. Tracer kinetic modelling for DCE-MRI quantification of subtle blood-brain barrier permeability. *NeuroImage* 2016; **125**, 446-55.

[27] H Xiong, P Yin, X Li, C Yang, D Zhang, X Huang and Z Tang. The features of cerebral permeability and perfusion detected by dynamic contrast-enhanced magnetic resonance imaging with Patlak model in relapsing-remitting multiple sclerosis. *Ther. Clin. Risk Manag.* 2018; **15**, 233-40.

[28] WD Rooney, X Li, MK Sammi, DN Bourdette, EA Neuwelt and CS Springer. Mapping human brain capillary water lifetime: High-resolution metabolic neuroimaging. *NMR Biomed.* 2015; **28**, 607-23.

[29] MJDL Pena, IC Pena, PG Garcia, ML Gavilan, N Malpica, M Rubio, RA Gonzalez and VMD Vega. Early perfusion changes in multiple sclerosis patients as assessed by MRI using arterial spin labeling. *Acta Radiol. Open* 2019; **8**, 205846011989421.

[30] J Chaganti, K Marripudi, LP Staub, CD Rae, TM Gates, KJ Moffat and BJ Brew. Imaging correlates of the blood-brain barrier disruption in HIV-associated neurocognitive disorder and therapeutic implications. *AIDS* 2019; **33**, 1843-52.

[31] Y Ohene, IF Harrison, PG Evans, DL Thomas, MF Lythgoe and JA Wells. Increased blood-brain barrier permeability to water in the aging brain detected using noninvasive multi-TE ASL MRI. *Magn. Reson. Med.* 2021; **85**, 326-33.

[32] A Chagnot, SR Barnes and A montagne. Magnetic resonance imaging of blood-brain barrier permeability in dementia. *Neuroscience* 2021; **474**, 14-29.

[33] Z Lin, S Sur, P Liu, Y Li, D Jiang, X Hou, J Darrow, JJ Pillai, S Yasar, P Rosenberg, M Albert, A Moghekar and H Lu. Blood-Brain barrier breakdown in relationship to alzheimer and vascular disease. *Ann. Neurol*. 2021; **90**, 227-38.

[34] RL Lee and KE Funk. Imaging blood-brain barrier disruption in neuroinflammation and Alzheimer's disease. *Front. Aging Neurosci.* 2023; **15**, 1144036.

[35] V Cuccurullo, GDD Stasio, ML Schilliro and L Mansi. Small-animal molecular imaging for preclinical cancer research: μPET and μSPECT. *Curr. Radiopharm.* 2016; **9**, 103-13.

[36] L Evangelista, AR Cervino, A Guttilla, F Zattoni, V Cuccurullo and L Mansi. ^{18}F-fluoromethylcholine or ^{18}F-fluoroethylcholine pet for prostate cancer imaging: Which is better? a literature revision. *Nucl. Med. Biol.* 2015; **42**, 340-8.

[37] M Grade, JAH Tamames, FB Pizzini, E Achten, X Golay and M Smits. A neuroradiologist's guide to arterial spin labeling MRI in clinical practice. *Neuroradiology* 2015; **57**, 1181-202.

[38] SP Cramer, HBW Larsson, MH Knudsen, HJ Simonsen, MB Vestergaard and U Lindberg. Reproducibility and optimal arterial input function selection in dynamic contrast-enhanced perfusion mri in the healthy brain. *J. Magn. Reson. Imaging* 2023; **57**, 1229-40.

[39] V Cuccurullo, GDD Stasio and GL Cascini. PET/CT in thyroid cancer - the importance of BRAF mutations. *Nucl. Med. Rev.* 2020; **23**, 97-102.

[40] A Ciarmiello, E Giovannini, M Meniconi, V Cuccurullo and MC Gaeta. Hybrid SPECT/ct imaging in neurology. Curr. Radiopharm. 2014; **7**, 5-11.

[41] C Kurz, L Walker, B Rauchmann and R Perneczky. Dysfunction of the blood-brain barrier in Alzheimer's disease: Evidence from human studies. *Neuropathol. Appl. Neurobiol.* 2022; **48**, e12782.

[42] S Mairinger, T Erker, M Muller and O Langer. PET and SPECT radiotracers to assess function and expression of ABC transporters *in vivo*. *Curr. Drug Metab.* 2011; **12**, 774-92.

[43] S Syvanen and J Eriksson. Advances in PET imaging of P-glycoprotein function at the blood-brain barrier. *ACS Chem. Neurosci.* 2013; **4**, 225-37.

[44] V Cuccurullo, F Cioce, A Sica, F Iasiello, R Capasso, G Gatta and G Rubini. Gastroenteric diseases in the third millennium: A rational approach to optimal imaging technique and patient selection. *Recenti Prog. Med.* 2012; **103**, 426-30.

[45] SL Kitson, V Cuccurullo, A Ciarmiello and L Mansi. Targeted therapy towards cancer-A perspective. *Anti Cancer Agents Med. Chem.* 2017; **17**, 311-7.

[46] L Mansi and V Cuccurullo. Diagnostic imaging in neuroendocrine tumors. *J. Nucl. Med.* 2014; **55**, 1576-7.

[47] KH Yoo, H Kang, J Oh, TH Lim, Y Cho, J Lee, SH Lee, S Jung, WY Kim, CH Sohn and BS Ko. Predicting acute brain lesions on magnetic resonance imaging in acute carbon monoxide poisoning: A multicenter prospective observational study. *Sci. Rep.* 2023; **13**, 22090.

[48] HJVD Haar, JFA Jansen, CRLPN Jeukens, S Burgmans, MAV Buchem, M Muller, PAM Hofman, FRJ Verhey, MJPV Osch and WH Backes. Subtle blood-brain barrier leakage rate and spatial extent: Considerations for dynamic contrast-enhanced MRI. *Med. Phys.* 2017; **44**, 4112-25.

[49] OZ Chi, X Liu and HR Weiss. Effects of cyclic GMP on microvascular permeability of the cerebral cortex. *Microvasc. Res.* 1999; **58**, 35-40.

[50] R Kim, SH Choi, TJ Yun, L Soon-Tae, P Chul-Kee, TM Kim, K Ji-Hoon, P Sun-Won, S Chul-Ho, P Sung-Hye and IH Kim. Prognosis prediction of non-enhancing T2 high signal intensity lesions in glioblastoma patients after standard treatment: Application of dynamic contrast-enhanced MR imaging. *Eur. Radiol.* 2017; **27**, 1176-85.

[51] TR Melzer, R Watts, MR MacAskill, JF Pearson, S Rueger, TL Pitcher, L Livingston, C Graham, R Keenan, A Shankaranarayanan, DC Alsop, JC Dalrymple-Alford and TJ Anderson. Arterial spin labelling reveals an abnormal cerebral perfusion pattern in Parkinson's disease. *Brain* 2011; **134**, 845-55.

[52] Y Meng, S Suppiah, K Mithani, B Solomon, ML Schwartz and N Lipsman. Current and emerging brain applications of MR-guided focused ultrasound. *J. Ther. Ultrasound* 2017; **5**, 26.